https://doi.org/10.5194/gmd-2023-44
Preprint. Discussion started: 12 April 2023

Geoscientific Model Development Discussions
Open Access
EGU

Modeling Collision-Coalescence in Particle Microphysics: Numerical Convergence of Mean and Variance of Precipitation in Cloud Simulations Using University of Warsaw Lagrangian Cloud Model (UWLCM) 2.1

Piotr Zmijewski, Piotr Dziekan, and Hanna Pawlowska
Institute of Geophysics, Faculty of Physics, University of Warsaw, Poland
Correspondence: Piotr Dziekan (pdziekan@fuw.edu.pl)

Abstract.

Numerical convergence of the collision-coalescence algorithm used in Lagrangian particle-based microphysics is studied in 2D simulations of an isolated Cumulus Congestus (CC) and in box simulations of collision-coalescence. Parameters studied are the time step for coalescence and the number of super-droplets per cell. Time step of $0.1\,\mathrm{s}$ gives converged droplet size distribution (DSD) in box simulations and converged mean precipitation in CC. Variances of the DSD and of precipitation are not sensitive to time step. In box simulations mean DSD converges for 10^3 super-droplets per cell, but variance of the DSD does not converge. In CC simulations mean precipitation converges for 5×10^3, but only in a strongly precipitating case. In cases with less precipitation, mean precipitation does not converge even for 10^5 super-droplet per cell. The result that more super-droplets are needed in CC simulations than in box simulations indicates that too large differences in the DSD between cells can reduce precipitation in cloud simulations. Variance in precipitation between independent CC runs is not affected by the number of super-droplets. This study suggests that parameters typically used in large-eddy simulations (LES) with particle microphysics can lead to underestimation of rain in lightly precipitating clouds.

1 Introduction

Particle microphysics (also know as Lagrangian particle-based microphysics, Lagrangian Cloud Model or super-droplet microphysics) is a class of Lagrangian methods for numerical modeling of cloud microphysics that has been developed in the last decade (Shima et al., 2009; Andrejczuk et al., 2010; Sölch and Kärcher, 2010; Riechelmann et al., 2012). In particle microphysics, numerical objects called super-droplets (SDs, also known as simulational particles) are used as proxies for hydrometeors. Similarly to the more common Eulerian bin models, particle models explicitly resolve evolution of the DSD. There are several advantages of particle models that make them a compelling alternative to bin models (Grabowski, 2020): lack of numerical diffusion, easy modeling of multiple hydrometeor attributes (e.g. chemical composition), scaling down to direct numerical simulations, among others. However, modeling of collision-coalescence has proven to be difficult in particle microphysics. A few algorithms have been developed to do this, see Unterstrasser et al. (2017) for a review. Out of these, the

https://doi.org/10.5194/gmd-2023-44
Preprint. Discussion started: 12 April 2023

Geoscientific Model Development Discussions

all-or-nothing (AON) algorithm from the Super-Droplet Method (SDM) of Shima et al. (2009) was shown to give the most accurate DSD in box simulations (Unterstrasser et al., 2017) and has been widely adopted (Hoffmann and Feingold, 2021; Dziekan et al., 2021; Unterstrasser et al., 2020; Arabas and Shima, 2013; Shima et al., 2020).

A recent study has found discrepancies in rain production between different particle models that use AON, although the models agree well in modeling condensational growth (Hill et al., 2023). This shows that better understanding of numerical convergence of AON is necessary before particle models can become the benchmark for microphysics modeling. Several studies have shown that AON is sensitive to the number of SDs, to the numerical time step and to the way SDs are initialized (Shima et al., 2009; Unterstrasser et al., 2017; Dziekan and Pawlowska, 2017; Dziekan et al., 2019; Unterstrasser et al., 2020). Detailed studies of numerical convergence of AON were done so far only in simulations of pure collision-coalescence in a box (Unterstrasser et al., 2017) and in a 1D column (Unterstrasser et al., 2020). It was found that criteria for convergence of AON are different in 1D than in box simulations. This shows that to confidently model precipitation in LES with particle microphysics, it is not sufficient to use parameters that give convergence in a box or a 1D column. The aim of this study is to better understand numerical convergence of AON in LES.

We begin with a study of numerical convergence of AON in simulations of collision-coalescence in a box model. Although a similar study was done by Unterstrasser et al. (2017), we believe that it is valuable to repeat it for a number of reasons. Firstly, our implementation of particle microphysics differs in details from that of Unterstrasser et al. (2017), so it may converge in a different way. Understanding convergence of our implementation in a box model is useful for planning convergence tests in more realistic simulations done afterwards. Secondly, we compare with a more detailed reference model than it was done in Unterstrasser et al. (2017). This allows us to study convergence not only of the mean DSD, but also of the variance of DSD. Lastly, we validate results of Unterstrasser et al. (2017).

Guided by box results, we proceed to study numerical convergence of AON in 2D simulations of isolated cumulus congestus. It is a much more realistic simulation than was used before for convergence tests of AON. The same processes are included as in a LES with the only difference being smaller dimensionality. The reason why we use 2D instead of 3D is that this decreases the required computational power and memory size, allowing us to study a broader range of parameters. AON is a stochastic algorithm, so it gives different realisations of collision-coalescence in independent simulation runs. LES runs often also differ due to random differences in initial conditions. These differences in initial conditions include random perturbations of thermodynamic variables (e.g. temperature and humidity) and random initialization of SD attributes. Stochasticity in AON, as well as in initial conditions, leads to differences in flow fields, what can strongly impact results. To isolate the effect of stochasticity of AON from stochasticity of initial conditions we use the same initial conditions in ensembles of simulations. Moreover, to facilitate studying convergence of AON, we use the same flow field for different simulations. This way flow field is not affected by different realisations of AON. We also perform reference ”dynamic” simulations with differences in initial conditions and without a prescribed flow field. This allows us to assess the importance of stochasticity of AON relatively to other sources of stochasticity in LES.

https://doi.org/10.5194/gmd-2023-44
Preprint. Discussion started: 12 April 2023

Geoscientific Model Development Discussions

We start with a presentation of the particle microphysics scheme with emphasis on AON and on the SD initialization procedure (section 2). Studies of numerical convergence of AON in box and in 2D simulations are presented in section 3 and in section 4, respectively. Conclusions for cloud modeling are discussed in section 5.

2 Particle microphysics

In Lagrangian particle micropyhysics methods particles in the air (aerosols, haze particles, cloud droplets, rain drops, ice particles) are represented by computational objects called super-droplets. In most cases, each SD represents a large number of identical real particles. The number of real particles a SD represents is called its multiplicity ξ (also known as weighting factor). Another commonly-used SD attribute is spatial position. Two additional attributes are useful for modeling warm microphysics: wet radius, which describes the total volume of a particle, and dry radius, which describes the volume of the dissolved matter. For most processes (advection, condensation, sedimentation), changes of SD attributes are described by the same equations that describe how single real particles are affected by these processes. However, it is not straightforward how to model collision-coalescence of SDs. In the next two sections we present parts of the microphysics model that are particularly important for modeling collision-coalescence.

2.1 Initialization of SD radii and multiplicities

Multiplicities and radii of SDs are initialized from a prescribed initial size distribution. In this section we describe common methods for doing this. The prescribed radius can either be wet or dry radius. We denote the initial number of SDs per grid cell with $N_{\mathrm{SD}}^{(\mathrm{init})}$.

In one initialization method, all SDs have same multiplicities and their initial radii are drawn from the distribution using inverse sampling (Shima et al., 2009; Hoffmann et al., 2015). Multiplicity is equal to the initial number of droplets in a cell divided by $N_{\mathrm{SD}}^{(\mathrm{init})}$. Following Unterstrasser et al. (2017), we refer to this method as ξ_{const}-init.

Another method of initialization is to divide the initial distribution into bins of equal sizes on a logarithmic scale. We denote the number of bins with $N_{\mathrm{SD}}^{(\mathrm{bin})}$. Within each bin we randomly select radius of a single SD, and its multiplicity follows from the initial distribution. It is not obvious what should be the choice of the leftmost and rightmost bin edges. Arabas et al. (2015) proposed to select edges so that multiplicities of SDs in the outermost bins is at least 1 (see Dziekan and Pawlowska (2017) for details of the algorithm). In this method bin edges depend on the volume of grid cells and, more importantly, on $N_{\mathrm{SD}}^{(\mathrm{bin})}$. When $N_{\mathrm{SD}}^{(\mathrm{bin})}$ is increased, the largest possible initial SD radius is decreased. To counter this, Dziekan and Pawlowska (2017) proposed to initialize additional SDs using inverse sampling from part of the distribution to the right of the rightmost bin. Note that the number of these additional SDs is rather small. In all simulations presented in this paper we have $N_{\mathrm{SD}}^{(\mathrm{bin})} \leq N_{\mathrm{SD}}^{(\mathrm{init})} \leq 1.01\, N_{\mathrm{SD}}^{(\mathrm{bin})}$. Following Dziekan and Pawlowska (2017), we will refer to this method as "constant SD"-init.

Instead of using the algorithm for finding bin edges, one can simply prescribe them. We call this method "constant SD" fixed-init. In this method no SDs are added to represent the part of the distribution to the right of the largest bin.

https://doi.org/10.5194/gmd-2023-44
Preprint. Discussion started: 12 April 2023


Geoscientific Model Development Discussions
Open Access
EGU

Unterstrasser et al. (2017) compared multiple methods of SD initialization and found that using bins to initialize radii (as in "constant SD"-init) is preferable because it requires the least SDs to correctly model collision-coalescence. In most of the simulations presented in this paper we use the "constant SD"-init. In section 4.7 we study sensitivity to SD initialization method.

2.2 Collision-coalescence of SDs: the AON algorithm

The AON algrithm, developed by Shima et al. (2009), is an algorithm for modeling collision-coalescence in Lagrangian particle microphysics. It is derived from the stochastic description of the collision-coalescence of particles (Gillespie, 1975). In this description, it is assumed that the probability of collision between a pair of particles is known. This probability is proportional to the coalescence kernel. AON is designed to give the correct expected number of collisions and to keep the number of SDs constant. The drawback of AON is that it gives a variance in the number of collisions larger than the real variance. The probability that a pair of super-droplets i and j collide during some time interval is:

$$P_{ij}^{(\mathrm{s})} = \max(\xi_i, \xi_j) P_{ij}\,, \tag{1}$$

where P_{ij} is the probability that two real particles with the same attributes as SDs i and j collide during the time interval. Coalescence of SDs i and j represents coalescence of $\min(\xi_i, \xi_j)$ pairs of real particles, each pair made of one particles represented by SD i and one particles represented by SD j. Probability of SD coalescence can be greater than one, in particular for long time steps. This represents multiple collisions between a SD pair within a single time step. Multiple collisions can be done only if the ratio of multiplicities of colliding SDs is sufficiently high (Shima et al., 2009). Note that in ξ_{const}-init it is not possible to have multiple collisions between a SD pair, because their multiplicities are equal. For this reason in our ξ_{const}-init simulations we adapt time step for coalescence to maintain collision probability below 1. The "constant SD"-init method typically gives large differences between multiplicities of SDs. Thanks to that multiple collisions per time step are possible and we use a constant time step for coalescence in this type of simulations.

In some implementations of AON, the number of super-droplet pairs tested for coalescence per time step is equal to $N_{\mathrm{SD}}\left(N_{\mathrm{SD}}-1\right)/2$, where N_{SD} is the number of SDs in a coalescence cell (the coalescence cell is typically equivalent to an Eulerian grid cell, Dziekan and Pawlowska (2017)). This is known as quadratic sampling (Unterstrasser et al., 2017, 2020). However, the original AON method of Shima et al. (2009) uses a technique called linear sampling, which is designed to speed up the algorithm. In linear sampling, $\lfloor N_{\mathrm{SD}}/2 \rfloor$ non-overlapping pairs of super-droplets are considered per time step. The notation $\lfloor x \rfloor$ represents the largest integer less than or equal to x. To obtain the correct expected number of collisions in linear sampling, the probability of collision between a pair of SDs is increased to:

$$P_{ij}^{(\mathrm{s,l})} = P_{ij}^{(\mathrm{s})} \frac{N_{\mathrm{SD}}\left(N_{\mathrm{SD}}-1\right)}{2} / \lfloor N_{\mathrm{SD}}/2 \rfloor\,. \tag{2}$$

Linear and quadratic sampling techniques were directly compared in Dziekan and Pawlowska (2017); Unterstrasser et al. (2020). Unterstrasser et al. (2020) showed that quadratic sampling converges for a longer time step than the linear sampling (Figure 6 b therein). Once converged, both techniques give the same mean and variance (Dziekan and Pawlowska, 2017;

https://doi.org/10.5194/gmd-2023-44
Preprint. Discussion started: 12 April 2023


Geoscientific Model Development Discussions
Open Access
EGU

Unterstrasser et al., 2020). Typically, the number of collision pairs tested per unit of time is smaller in linear sampling than in quadratic sampling, despite the shorter time steps. Moreover, in linear sampling all collision pairs can be computed in parallel because they are non-overlapping. For these reasons, we use linear sampling in this work.

3 Box simulations

We model collision-coalescence of droplets in a well-mixed box. For simplicity, we use r to denote wet radius in this section, as the dry radius is not important for collision-coalescence.We analyze the mean $\langle m \rangle$ and standard deviation $\sigma(m)$ of the mass density function $m(\ln r)$. The mass density function is such that $m(\ln r)\, d\ln r$ is the mass of droplets per unit volume in the size range from $\ln r$ to $\ln r + d\ln r$. The initial distribution of r is exponential in volume with $15\,\mu\mathrm{m}$ mean wet radius and $142\,\mathrm{cm}^{-3}$ droplet concentration, what gives $2\,\mathrm{g\,m}^{-3}$ liquid water content. This distribution was used in Onishi et al. (2015); Dziekan and Pawlowska (2017). The box volume is around $0.45\,\mathrm{m}^3$ and it initially contains 64 million droplets. Simulations are run for $300\,\mathrm{s}$. We use a gravitational coalescence kernel with collision efficiencies from Hall (1980) and from Davis (1972).

Three types of collision-coalescence models are compared: AON algorithm, one-to-one simulations and the stochastic coalescence equation (SCE). AON is discussed in section 2. One-to-one simulations are particle simulations with $\xi = 1$, i.e. each real droplet is explicitly modeled. We use ξ_{const}-init and linear sampling in one-to-one simulations. One-to-one simulations produce a realization in agreement with the master equation (Dziekan and Pawlowska, 2017). As such, they are the most fundamental type of simulation used and are considered to produce reference results. SCE is an equation for time evolution of the average DSD. It is typically used to model collision-coalescence in bin models. Dziekan and Pawlowska (2017) showed that the SCE gives correct average results for droplet populations greater than 10^7, so it should be valid in the box simulation with 6.4×10^7 droplets discussed in this paper. We solve SCE with the Bott (1997) flux method with bin scaling parameter $\alpha = 2^{1/10}$ and time step $0.1\,\mathrm{s}$. These parameters were found to give converged results.

One-to-one and AON simulations are stochastic. We run ensembles of these simulations and calculate $\langle m \rangle$ and $\sigma(m)$ from the ensembles. The SCE is deterministic and does not explicitly model variance of the DSD. However, Gillespie (1975) estimated the variance of the number of droplets in a given size range to be equal to the number of droplets in this size range. We validate this estimate by comparing it with one-to-one results.

3.1 Results of box simulations

First we check how numerical time step Δt_{coal} affects AON simulations with $N_{\mathrm{SD}}^{(\mathrm{bin})} = 10^2$, what is the number of SDs typical for LES. In fig. 1 we show DSDs at the end of the simulation for different time step lengths. There are no differences in $\langle m \rangle$ between $\Delta t_{\mathrm{coal}} = 0.1\,\mathrm{s}$ and $\Delta t_{\mathrm{coal}} = 0.01\,\mathrm{s}$. Using $\Delta t_{\mathrm{coal}} = 1\,\mathrm{s}$ results in too large $\langle m \rangle$ for the largest droplets. $\Delta t_{\mathrm{coal}} = 10\,\mathrm{s}$ gives yet larger $\langle m \rangle$ for the largest droplets and also a decrease in $\langle m \rangle$ for droplets with radii between $40\,\mu\mathrm{m}$ and $100\,\mu\mathrm{m}$. Regarding fluctuations, we see that differences in $\sigma(m)$ correspond to differences in $\langle m \rangle$, e.g. too large $\langle m \rangle$ for largest droplets also gives too large $\sigma(m)$ for largest droplets. From this test we conclude that mean DSD converges for $\Delta t_{\mathrm{coal}} = 0.1\,\mathrm{s}$ and that fluctuations in DSD are not sensitive to Δt_{coal}.

https://doi.org/10.5194/gmd-2023-44
Preprint. Discussion started: 12 April 2023

Geoscientific Model Development Discussions

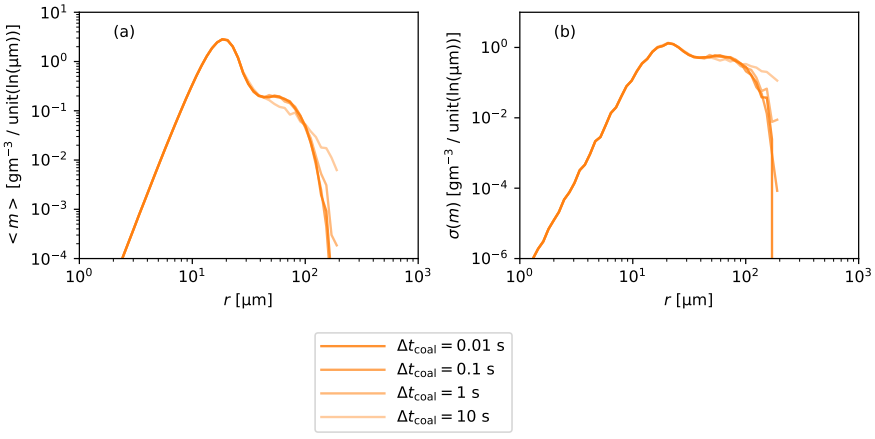

Figure 1. (a) Mean and (b) standard deviation of the mass density function m for $N_{\mathrm{SD}}^{(\mathrm{bin})} = 10^2$ box simulations at $t = 300\,\mathrm{s}$ for different time step lengths.

Next we check how results are affected by the number of SDs for $\Delta t_{\mathrm{coal}} = 0.1\,\mathrm{s}$. In fig. 2 we show DSDs at the beginning and at the end of an AON simulation for different $N_{\mathrm{SD}}^{(\mathrm{bin})}$. Results of one-to-one simulations and of the SCE are plotted for reference. The initial $\langle m \rangle$ is very well represented for all methods of radius initialization and agrees well with the SCE initialization (fig. 2 (a)). The initial $\sigma(m)$ in decreases approximately linearly with increasing $N_{\mathrm{SD}}^{(\mathrm{bin})}$ (fig. 2 b). $N_{\mathrm{SD}}^{(\mathrm{bin})} = 10^5$ gives smaller initial $\sigma(m)$ than one-to-one despite much higher number of SDs in the latter (6.4×10^7). The reason for this are the differences in the radius initialization procedure. The mean DSD at the end of the simulation does not significantly differ between different types of simulations with the exception of $N_{\mathrm{SD}}^{(\mathrm{bin})} = 10$, which gives too little droplets with radii between $30\,\mu\mathrm{m}$ and $130\,\mu\mathrm{m}$, and too many droplets with $r > 130\,\mu\mathrm{m}$ (fig. 2 c). Fluctuations in DSD at the end of AON simulations decrease with increasing $N_{\mathrm{SD}}^{(\mathrm{bin})}$ (fig. 2 d). Standard deviation $\sigma(m)$ is proportional to $\sqrt{N_{\mathrm{SD}}^{(\mathrm{bin})}}^{-1}$, in particular for $10^3 \leq N_{\mathrm{SD}}^{(\mathrm{bin})} \leq 10^5$. Even for $N_{\mathrm{SD}}^{(\mathrm{bin})} = 10^5$ the $\sigma(m)$ in AON is much larger than the reference one-to-one result. It is seen that $\sigma(m)$ estimated from the SCE as the square root of the number of droplets is larger than the one-to-one result, but much closer to it than $\sigma(m)$ in AON with $N_{\mathrm{SD}}^{(\mathrm{bin})} = 10^5$. Note that LES cells contain many more droplets than our modeled box. Therefore in LES the difference between the expected $\sigma(m)$ and the $\sigma(m)$ modeled with the AON algorithm for computationally feasible values of $N_{\mathrm{SD}}^{(\mathrm{bin})}$ is larger than in the presented box simulations.

Differences in $\langle m \rangle$ between simulations for different combinations of $N_{\mathrm{SD}}^{(\mathrm{bin})}$ and of Δt_{coal} may potentially lead to differences in the mean amount of rain in LES with Lagrangian particle microphysics. To have a better view of this issue we plot differences between $\langle m \rangle$ in one-to-one simulations and $\langle m \rangle$ in AON simulations with different $N_{\mathrm{SD}}^{(\mathrm{bin})}$ (fig. 3). In the plot, $\langle m \rangle$ is multiplied by the terminal velocity to get the sedimentation mass flux of droplets of given size. This analysis confirms that results converge for $\Delta t_{\mathrm{coal}} = 0.1\,\mathrm{s}$, irrespective of $N_{\mathrm{SD}}^{(\mathrm{bin})}$ (fig. 3 a-c). Longer time steps result in underestimation of the sedimentation flux for droplets with radii between around 40 and around 120 microns and in overestimation of sedimentation flux for other droplets. Regarding convergence with $N_{\mathrm{SD}}^{(\mathrm{bin})}$, we find that AON results agree with one-to-one for

https://doi.org/10.5194/gmd-2023-44
Preprint. Discussion started: 12 April 2023

Geoscientific Model Development Discussions
Open Access
EGU

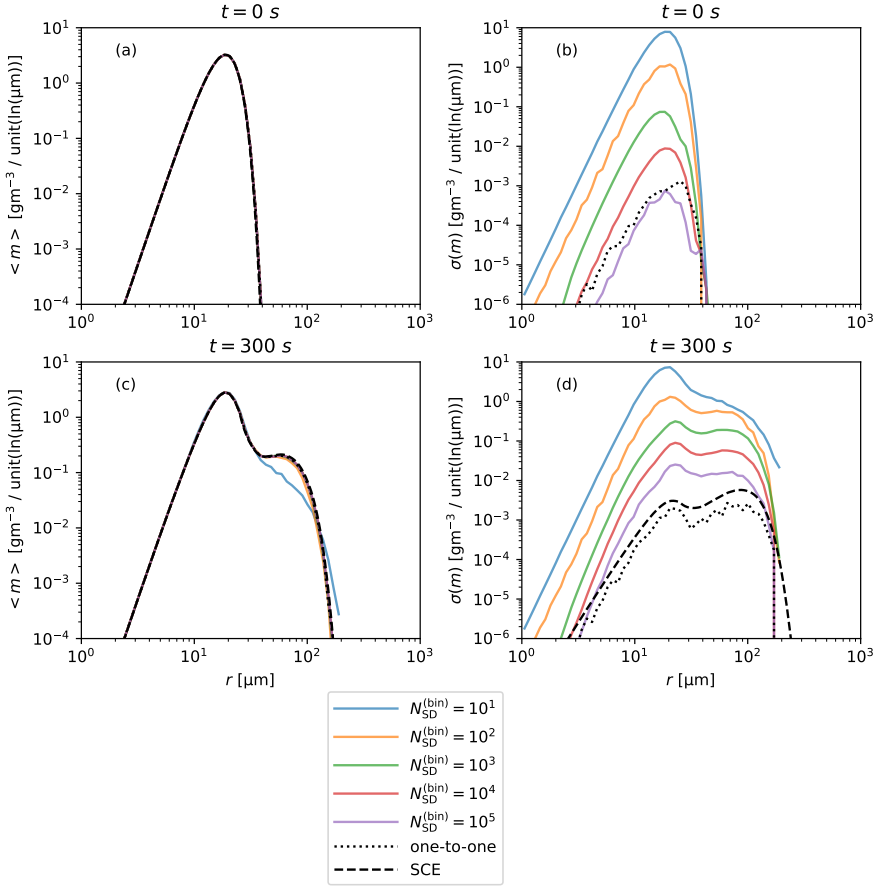

Figure 2. Mean and standard deviation of the mass density function m from box simulations at $t = 0\,\mathrm{s}$ (a-b) and at $t = 300\,\mathrm{s}$ (c-d). Two types of Lagrangian simulations (SDM with $\Delta t_{\mathrm{coal}} = 10\,\mathrm{s}$ and for different $N_{\mathrm{SD}}^{(\mathrm{bin})}$; one-to-one simulations) and the SCE are compared.

$N_{\mathrm{SD}}^{(\mathrm{bin})} \geq 10^3$ (fig. 3 d). For $N_{\mathrm{SD}}^{(\mathrm{bin})} = 10$ the mass flux is overestimated for $r < 30\,\mu\mathrm{m}$ and $r > 130\,\mu\mathrm{m}$ and underestimated for $30\,\mu\mathrm{m} < r < 130\,\mu\mathrm{m}$. Using $N_{\mathrm{SD}}^{(\mathrm{bin})} = 10^2$ underestimates mass flux for $r > 50\,\mu\mathrm{m}$.

Initialization of droplet radii in Lagrangian particle microphysics is often stochastic (Shima et al., 2009; Unterstrasser et al., 2017; Dziekan and Pawlowska, 2017). It is a source of random differences between simulations that is separate from the stochastic collision-coalescence algorithm. We want to check how important are these two different sources of randomness for variance in the modeled DSD. We run ensembles of simulations that do not differ in the initial DSD, but differ only in the realization of collision-coalescence. Comparison of these simulations with simulations that differ both in the initial DSD and the realization of collision-coalescence is shown in fig. 4. The comparison is done for one-to-one simulations and for AON simulations with $N_{\mathrm{SD}}^{(\mathrm{bin})} = 100$. The initial $\langle m \rangle$ agrees well for all types of simulations (fig. 4 a). As expected, the initial $\sigma(m)$ is equal to zero for simulations without randomness in the initial DSD (fig. 4 b). At the end of the simulation $\langle m \rangle$ agrees well between simulations with and without randomness in initial DSD (fig. 4 c). For droplets with $r > 20\,\mu\mathrm{m}$, $\sigma(m)$ at the end of

https://doi.org/10.5194/gmd-2023-44
Preprint. Discussion started: 12 April 2023

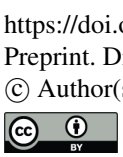

Geoscientific Model Development Discussions
Open Access
EGU

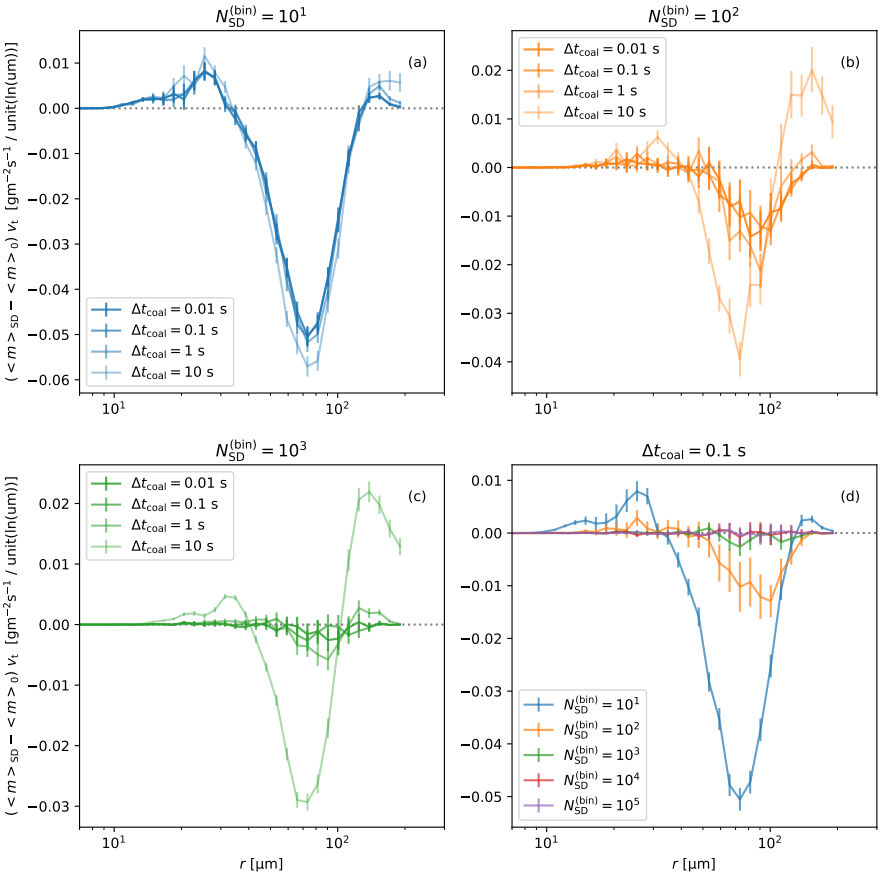

Figure 3. Differences between $\langle m \rangle$ from SDM ($\langle m \rangle_{\mathrm{SD}}$) and one-to-one ($\langle m \rangle_0$) Lagrangian microphysics, multiplied by terminal velocity v_t. Results of box model simulations at $t = 300\,\mathrm{s}$. Vertical error bars show the $95\,\%$ confidence interval.

the simulation is also not sensitive to randomness in the initial DSD (fig. 4 d). Lack of randomness in the initial DSD results in slightly smaller $\sigma(m)$ for $r < 20\,\mu\mathrm{m}$, $\sigma(m)$ (fig. 4 d). Considering that collision-coalescence is responsible for formation of large droplets and that smaller droplets are formed by condensation we conclude that the randomness in the initial DSD is not important for mean nor fluctuations in large droplet production.

3.2 Summary of box simulations and comparison with previous studies

Box simulations of collision-coalescence with AON show convergence of $\langle m \rangle$ for $\Delta t_{\mathrm{coal}} \leq 0.1\,\mathrm{s}$, irrespective of $N_{\mathrm{SD}}^{(\mathrm{bin})}$, and for $N_{\mathrm{SD}}^{(\mathrm{bin})} \geq 10^3$. The standard deviation $\sigma(m)$ is not sensitive to Δt_{coal}, but decreases with increasing $N_{\mathrm{SD}}^{(\mathrm{bin})}$. Variance of the number of droplets in a size bin is approximately equal to the number of droplets. This relationship could be used to model the stochastic nature of collision-coalescence in bin microphysics.

https://doi.org/10.5194/gmd-2023-44
Preprint. Discussion started: 12 April 2023

Geoscientific Model Development Discussions

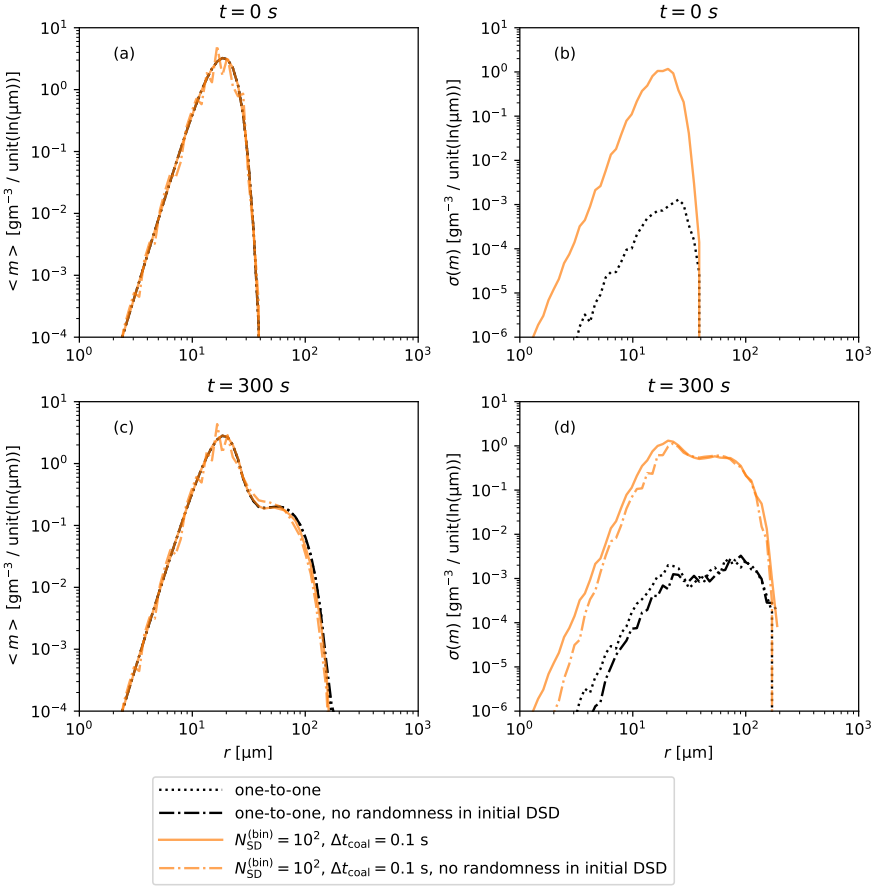

Figure 4. As in fig. 2, but comparing ensembles of simulations with and without randomness in the initial DSD.

Box model tests of the mean DSD in the AON algorithm were previously done by Shima et al. (2009); Unterstrasser et al. (2017). Unterstrasser et al. (2020) did column simulations and some of them did not include sedimentation, which is equivalent to box simulations. Shima et al. (2009) found relatively good agreement with the SCE for $\Delta t_{\mathrm{coal}} = 0.1\,\mathrm{s}$ and for $N_{\mathrm{SD}}^{(\mathrm{bin})} \approx 2 \times 10^6$. The time step requirement is the same as found in this work, but the required $N_{\mathrm{SD}}^{(\mathrm{bin})}$ is much higher. The latter is probably because Shima et al. (2009) used the constant multiplicity initialization, which was found by Unterstrasser et al. (2017) to require many more SDs than their "singleSIP" initialization, which is similar to our constant SD initialization.

Using the "singleSIP" initialization, Unterstrasser et al. (2017) showed that results are close to converging for $\Delta t_{\mathrm{coal}} = 1\,\mathrm{s}$ (fig. 19 therein, first column, second row), although shorter time steps were not considered. An important difference between this work and Unterstrasser et al. (2017) is that the latter used quadratic sampling. Differences between linear and quadratic sampling methods are discussed in section 2.2. Regarding convergence with $N_{\mathrm{SD}}^{(\mathrm{bin})}$, Unterstrasser et al. (2017) found convergence for $N_{\mathrm{SD}}^{(\mathrm{bin})} \geq 10^3$ (Fig. 19 therein, second column; there $\kappa = 200$ corresponds to $N_{\mathrm{SD}}^{(\mathrm{bin})} \approx 10^3$) and Unterstrasser et al. (2020) did not find convergence for up to $N_{\mathrm{SD}}^{(\mathrm{bin})} = 10^3$ (Fig. 6 a therein). Convergence tests in Unterstrasser et al. (2017, 2020)

https://doi.org/10.5194/gmd-2023-44
Preprint. Discussion started: 12 April 2023


Geoscientific Model Development Discussions

were based on comparing the 0-th, 2-nd and 3-rd moments of the DSD (it was most difficult to obtain convergence of the 0-th moment). These tests are good for looking for large errors, but do not reveal smaller differences in the DSD. Small differences can nevertheless be important for rain formation, which depends on the large end of the DSD. To illustrate this, we consider our box simulations for $N_{\mathrm{SD}}^{(\mathrm{bin})} = 10^2$. In these simulations, $\Delta t_{\mathrm{coal}} = 10\,\mathrm{s}$ gives significantly different large end of the DSD than $\Delta t_{\mathrm{coal}} = 0.1\,\mathrm{s}$ (fig. 1), but the difference in the 0-th moment is only around $0.5\,\%$.

The AON implementation from the *libcloudph++* library, which is the implementation used in this paper, was also used in box simulations in Dziekan and Pawlowska (2017). That paper discussed convergence of $t_{10\%}$, the time after which $10\,\%$ of cloud mass is turned into rain mass. Dziekan and Pawlowska (2017) found that for $\Delta t_{\mathrm{coal}} = 1\,\mathrm{s}$ mean $t_{10\%}$ converges for $N_{\mathrm{SD}}^{(\mathrm{bin})} \geq 10^3$ (Fig. 4 therein). Dziekan and Pawlowska (2017) also showed that standard deviation of $t_{10\%}$ decreases linearly with the square root of $N_{\mathrm{SD}}^{(\mathrm{bin})}$ (Fig. 5 therein). This is in agreement our observation that $\sigma(m)$ is proportional to $\sqrt{N_{\mathrm{SD}}^{(\mathrm{bin})}}^{-1}$ and with the theoretical prediction from Shima et al. (2009) (Sec. 4.1.4 therein).

4 2D Cumulus Congestus Simulations

In this section we analyze AON in a two-dimensional simulation of an isolated cumulus congestus cloud. Conclusions about convergence of AON in box simulations that were presented in the previous section do not necessarily apply to higher dimensional simulations or simulations that include more processes affecting the DSD (e.g. condensational growth). For example, Unterstrasser et al. (2020) found that it is easier to reach convergence in a one-dimensional column simulation than in a box simulation. Based on the fact that in box simulations $\langle m \rangle$ converges for large $N_{\mathrm{SD}}^{(\mathrm{bin})}$, we can expect that precipitation in the CC simulation also converges for large $N_{\mathrm{SD}}^{(\mathrm{bin})}$. It is more difficult to assess what errors can be expected in precipitation in the CC simulation due to artificially large variance in AON, which is illustrated by the lack of convergence of $\sigma(m)$ in box simulations. Too large variance in AON may result in too large differences in the DSD between cells. This might affect precipitation averaged over the entire cloud, because there is mixing between cells. Too large variance may also cause too large differences in precipitation between independent simulation runs. However, it is possible that in cloud simulations spatial and temporal variability of DSD is more susceptible to other factors, e.g. changes in relative humidity. Then, too large variability in AON would not be a problem. Variance in the number of collisions is proportional to $N_{\mathrm{SD}}^{(\mathrm{bin})}$ (see section 3). Doing CC simulations for different values of $N_{\mathrm{SD}}^{(\mathrm{bin})}$ allows us to study how the artificially large variance in AON affects simulations, even though it is not possible to have $N_{\mathrm{SD}}^{(\mathrm{bin})}$ large enough for the variance to converge.

4.1 LES model

The CC simulations are done with the University of Warsaw Lagrangian Cloud Model (UWLCM). UWLCM is a LES tool that allows 2D and 3D simulations with Lagrangian particle (or Eulerian bulk) microphysics. Thermodynamic variables (potential temperature, water vapor mixing ratio, velocity) are modeled in an Eulerian manner. The Lipps-Hemler anelastic approximation (Lipps and Hemler, 1982) is used to filter acoustic waves. For spatial discretization of Eulerian variables, the staggered Arakawa-C grid (Arakawa and Lamb, 1977) is used. The finite-difference method is used to solve equations for Eulerian

https://doi.org/10.5194/gmd-2023-44
Preprint. Discussion started: 12 April 2023


Geoscientific Model Development Discussions
Open Access
EGU

variables. The multidimensional positive-definite advection transport algorithm (MPDATA) (Smolarkiewicz, 2006) is used to model transport of Eulerian variables. The model uses the generalized conjugate residual solver (Smolarkiewicz and Margolin, 2000) to solve the pressure disturbance. In this paper, subgrid-scale transport is modeled using the implicit LES approach (Grinstein et al., 2007). A more detailed description of UWLCM can be found in Dziekan et al. (2019); Dziekan and Zmijewski (2022).

4.2 Simulation setup

We use an isolated cumulus congestus modeling setup that was one of the cases studied at the International Cloud Modeling Workshop 2020. It is an adaptation of the setup developed by Lasher-Trapp et al. (2001). The computational domain is 12 km in horizontal and 10 km in vertical. Vertical profiles come from a conditionally unstable sounding from the Small Cumulus Microphysics Study field campaign. Initial potential temperature and water vapor mixing ratio fields are randomly perturbed below $1\,\mathrm{km}$ altitude. Perturbation amplitudes are $0.025\,\mathrm{g\,kg^{-1}}$ and $0.01\,\mathrm{K}$. For the first hour, surface fluxes are uniform: $0.04\,\mathrm{g\,kg^{-1}\,m\,s^{-1}}$ latent heat flux and $0.1\,\mathrm{K\,m\,s^{-1}}$ sensible heat flux. Afterwards, surface fluxes have a Gaussian distribution centered at the middle of the domain with maxima three times larger than the uniform flux from the first hour and with half width of $1.7\,\mathrm{km}$. The momentum surface flux is given by a constant friction velocity $0.28\,\mathrm{m\,s^{-1}}$. The total simulation time is 3 hours. The lateral boundaries are periodic, and the upper boundary is free-slip rigid-lid. We use an aerosol distribution based on observations from the RICO campaign (VanZanten et al., 2011). The distribution is made of two log-normal modes. The first (second) mode parameters are: number concentration $90\,\mathrm{cm^{-3}}$ ($15\,\mathrm{cm^{-3}}$), geometric mean radius $0.03\,\mu\mathrm{m}$ ($0.14\,\mu\mathrm{m}$) and geometric standard deviation 1.28 (1.75). Aerosol type is ammonium bisulfate. We model these relatively clean conditions in order to have significant amount of precipitation, which is the focus of this study. A gravitational coalescence kernel is used with collision efficiencies from Hall (1980) for large droplets and from Davis (1972) for small droplets. The coalescence efficiency is set to one. There is no droplet breakup. Terminal velocities are calculated using a formula of Khvorostyanov and Curry (2002). Model time step is $0.5\,\mathrm{s}$, time step for condensation is $0.1\,\mathrm{s}$ and cell size is $100\,\mathrm{m}$ in each direction.

We use 2D instead of 3D LES, because it allows us to study much larger values of $N_{\mathrm{SD}}^{(\mathrm{bin})}$. The same processes are modeled in 2D as in 3D, e.g. condensation, advection, sedimentation, collision-coalescence, etc. In 2D the modeled flow field has different characteristics than in 3D, but we do not expect this to affect numerical convergence of the collision-coalescence algorithm. We expect to see more variability between simulation runs in 2D than there would be in 3D, because of a much smaller number of spatial cells. However, we think that the way this variability is affected by parameters of the microphysics scheme in 2D is representative of how it would be affected in 3D.

4.3 Simulation strategy

Typically in LES there is a random perturbation of initial conditions, e.g. of temperature and humidity. In LES with particle microphysics, initial conditions may also differ in SD attributes, because they are often randomly initialized. This randomness in initial conditions leads to differences in results between simulation runs, independently of AON. To understand the role of AON we isolate its effect by comparing dynamic and kinematic simulations. In dynamic simulations pressure equation is

https://doi.org/10.5194/gmd-2023-44
Preprint. Discussion started: 12 April 2023


Geoscientific Model Development Discussions

solved, meaning that different realisations of microphysics lead to different flow fields. In kinematic simulations, flow field is prescribed. Our strategy is to run an ensemble of dynamic (D) simulations with random differences in initial conditions. We consider this ensemble as a control group, because this is the way LES is usually done. From dynamic simulations, we select three realizations: one with little, one with medium and one with high amount of rain (LR, MR and HR, respectively). Flow fields from these simulations are used to run ensembles of kinematic simulations. Sizes of ensembles are given in the Supplement. In these kinematic simulations initial conditions do not change within an ensemble. Therefore any variability within a kinematic ensemble is solely caused by AON. In our analysis, we focus on ensemble mean $\langle P \rangle$ and standard deviation $\sigma(P)$ of accumulated surface precipitation at the end of a simulation. We look at precipitation, because it is an important observable that strongly depends on collision-coalescence of droplets. In each simulation a single cloud is modeled and it precipitates for a short period of time, so we decided that it is sufficient to study accumulated precipitation. To test the convergence of AON, we check how $\langle P \rangle$ and $\sigma(P)$ are affected by $N_{\mathrm{SD}}^{(\mathrm{bin})}$ and by Δt_{coal}. For estimating errors of ensemble statistics we use the following formulas. The standard error of $\langle P \rangle$ is:

$$\mathrm{se}(\langle P \rangle) = \frac{\sigma(P)}{\sqrt{n}}. \tag{3}$$

The standard error of $\sigma(P)$ is (Rao, 1973, p.438):

$$\mathrm{se}(\sigma(P)) = \frac{1}{2\sigma(P)} \sqrt{\frac{1}{n}\left(\left\langle (P - \langle P \rangle)^4 \right\rangle - \frac{n-3}{n-1}\sigma(P)^4\right)}. \tag{4}$$

The $95\,\%$ confidence interval of $\langle P \rangle$ is:

$$\mathrm{CI}_{95\%}\left(\langle P \rangle\right) = \left[\langle P \rangle - 1.96 \cdot \mathrm{se}\left(\langle P \rangle\right), \langle P \rangle + 1.96 \cdot \mathrm{se}\left(\langle P \rangle\right)\right]. \tag{5}$$

The $95\,\%$ confidence interval of $\sigma(P)$ is (Sheskin, 2020, p.217):

$$\mathrm{CI}_{95\%}\left(\sigma(P)\right) = \left[\sigma(P)\sqrt{\frac{n-1}{f\left(0.975, n-1\right)}}, \sigma(P)\sqrt{\frac{n-1}{f\left(0.025, n-1\right)}}\right], \tag{6}$$

where $f(x, y)$ is the inverse CDF of the chi-squared distribution.

4.4 Generating velocity fields for kinematic simulations

We start with running a large number of dynamic simulations in order to find three velocity fields that are expected to give significantly different amounts of rain. These velocity fields will later be used in kinematic simulations. In a single dynamic simulation, the amount of precipitation depends not only on the realized flow field, but also on the realization of the AON algorithm. This means that rain from a single dynamic simulation is not representative of the expected amount of rain from a series of simulations with the same velocity field. To be sure that we select velocity fields that will give different amounts of rain, first we chose a candidate velocity fields based on the amount of rain in the single dynamic run, and then we run 20 kinematic simulations and use the average from these simulations to calculate the expected amount of rain. Based on this

https://doi.org/10.5194/gmd-2023-44
Preprint. Discussion started: 12 April 2023

Geoscientific Model Development Discussions
Open Access
EGU

procedure, we selected the three velocity fields for kinematic simulations: LR, MR and HR. In fig. 5 we show a frequency histogram of P from the ensemble of dynamic simulations.

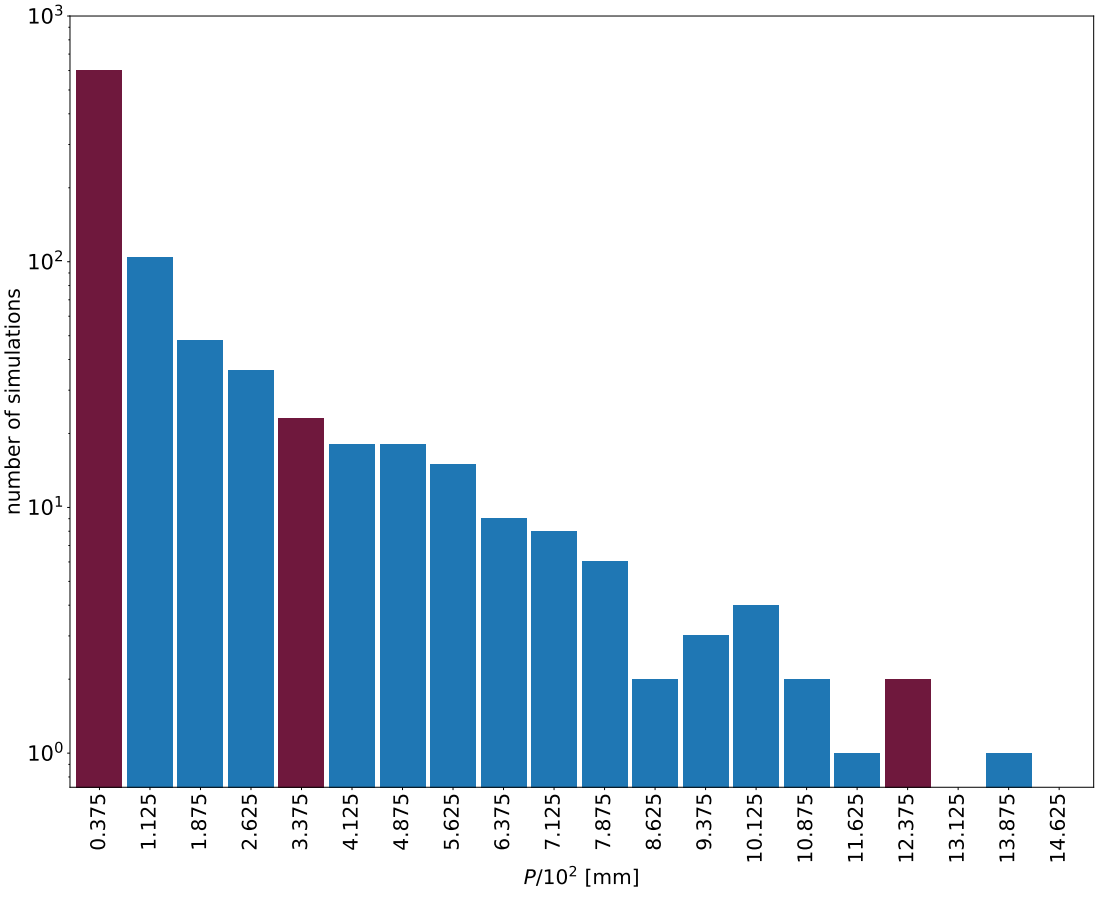

Figure 5. Frequency histogram of P from the ensemble of dynamic simulations with $N_{\mathrm{SD}}^{(\mathrm{bin})} = 10^2$. Horizontal axis is bin center. Bin width is $7.5 \cdot 10^{-3}\mathrm{mm}$. Vertical axis is the number of simulations with P within a bin. The bins in burgundy colour show the expected rain amount for LR, MR and HR velocity fields (left to right).

4.5 Time series

In this section we discuss temporal development of general cloud properties in the D, LR, MR and HR scenarios. This is done to give the readers an idea about how the modeled cloud develops. Time series of cloud top height (CTH), cloud cover (cc), cloud water path (CWP), rain water path (RWP) and precipitation are plotted in fig. 6. The results are ensemble averages. For brevity, only results for $N_{\mathrm{SD}}^{(\mathrm{bin})} = 100$ are shown. Time series for other values of $N_{\mathrm{SD}}^{(\mathrm{bin})}$ are similar and are available as supplemental information.

https://doi.org/10.5194/gmd-2023-44
Preprint. Discussion started: 12 April 2023

Geoscientific Model Development Discussions

Time series of CTH, cc and CWP are smoother in dynamic than in kinematic simulations. In dynamic simulations there are differences between simulation runs in the moment cloud starts to develop. When averaged over simulation runs, the results are smooth. In kinematic simulations, cloud develops in a very similar way in all simulations within an ensemble. Therefore the ensemble average resembles a single dynamic simulation in that it changes significantly at short time scales. This illustrates that, unsurprisingly, CTH, cc and CWP are more sensitive to the air flow than to the realization of collision-coalescence.

In all scenarios cloud starts to develop at around $1500\,\mathrm{s}$. Afterwards it deepens with time, reaching maximum cc at around $5500\,\mathrm{s}$ and maximum CWP at around $7000\,\mathrm{s}$. In kinematic scenarios, rain appears shortly after CWP reaches its maximum. The cloud almost entirely disappears at around $9500\,\mathrm{s}$ (CWP close to 0). A second cloud starts to develop near the end of the simulation, indicated by an increase in CWP. The differences in rain between LR, MR and HR are explained by differences in CWP, with highest CWP giving most rain. In MR and in HR, CWP steadily increases until rain is formed. The difference is that CWP and CTH reach higher values in HR than in MR. In LR there are multiple local maxima of CWP, each of them smaller than the maxima in MR and HR.

4.6 Numerical convergence of precipitation

In this section we discuss how ensemble statistics of accumulated precipitation at the end of a simulation depend on parameters of the collision-coalescence model. Figure 7 shows sensitivity to Δt_{coal}, the time step with which coalescence is modeled. We find no statistically significant impact of Δt_{coal} on $\langle P \rangle$ or on $\sigma(P)$ for $\Delta t_{\mathrm{coal}} \leq 0.5\,\mathrm{s}$. Sensitivity to time step was tested only for $N_{\mathrm{SD}}^{(\mathrm{bin})} = 100$, because box simulations showed that results converge for the same value of Δt_{coal}, independent of the value of $N_{\mathrm{SD}}^{(\mathrm{bin})}$. Sensitivity to $N_{\mathrm{SD}}^{(\mathrm{bin})}$ is discussed in the subsequent sections.

4.6.1 Convergence of $\langle P \rangle$ with $N_{\mathrm{SD}}^{(\mathrm{bin})}$

Mean precipitation for differing number of SDs is shown in fig. 8. We find that $\langle P \rangle$ varies with $N_{\mathrm{SD}}^{(\mathrm{bin})}$ in a non-trivial way, similar in all four scenarios. Mean precipitation is the highest for $N_{\mathrm{SD}}^{(\mathrm{bin})} = 10$. Then, there is a large decrease in $\langle P \rangle$ when $N_{\mathrm{SD}}^{(\mathrm{bin})}$ is increased from 10 to 50. A minimum of $\langle P \rangle$ is found between $N_{\mathrm{SD}}^{(\mathrm{bin})} = 50$ and $N_{\mathrm{SD}}^{(\mathrm{bin})} = 10^3$, depending on the scenario. Beyond this minimum, $\langle P \rangle$ slowly increases (see subplots e-h). Uncertainties in $\langle P \rangle$ are large (in particular in D) and the 95% confidence intervals often overlap. However, center of the confidence interval systematically increases with $N_{\mathrm{SD}}^{(\mathrm{bin})}$ in D, LR and MR (subplots e-g). The fact that this happens in three independent scenarios is an indication that the increase of $\langle P \rangle$ with $N_{\mathrm{SD}}^{(\mathrm{bin})}$ for $N_{\mathrm{SD}}^{(\mathrm{bin})} \geq 10^3$ is not a just a random, statistically insignificant effect. In HR, unlike in the other scenarios, there is evidence for convergence of $\langle P \rangle$ for $N_{\mathrm{SD}}^{(\mathrm{bin})} \geq 5 \times 10^3$. Centers of confidence intervals are at similar positions for $N_{\mathrm{SD}}^{(\mathrm{bin})} = 5 \times 10^3$, $N_{\mathrm{SD}}^{(\mathrm{bin})} = 4 \times 10^4$ and for $N_{\mathrm{SD}}^{(\mathrm{bin})} = 10^5$ and the intervals are small. For $N_{\mathrm{SD}}^{(\mathrm{bin})} = 10^4$ the confidence interval center is lower, but the interval is large and covers centers of neighbouring intervals.

Changes of $\langle P \rangle$ for $N_{\mathrm{SD}}^{(\mathrm{bin})} \leq 10^3$ are consistent with results of box simulations of collision-coalescence and of CC simulations without collision-coalescence. In box simulations there are errors in the mean DSD for $N_{\mathrm{SD}}^{(\mathrm{bin})} \leq 10^3$. In CC simulations without collision-coalescence, which are presented in the Supplement, there are deviations in time series for $N_{\mathrm{SD}}^{(\mathrm{bin})} \leq 10^3$. This shows that $N_{\mathrm{SD}}^{(\mathrm{bin})} \leq 10^3$, and $N_{\mathrm{SD}}^{(\mathrm{bin})} = 10$ in particular, gives errors in modeling of condensational growth.

https://doi.org/10.5194/gmd-2023-44
Preprint. Discussion started: 12 April 2023

Geoscientific Model Development
Discussions
Open Access
EGU

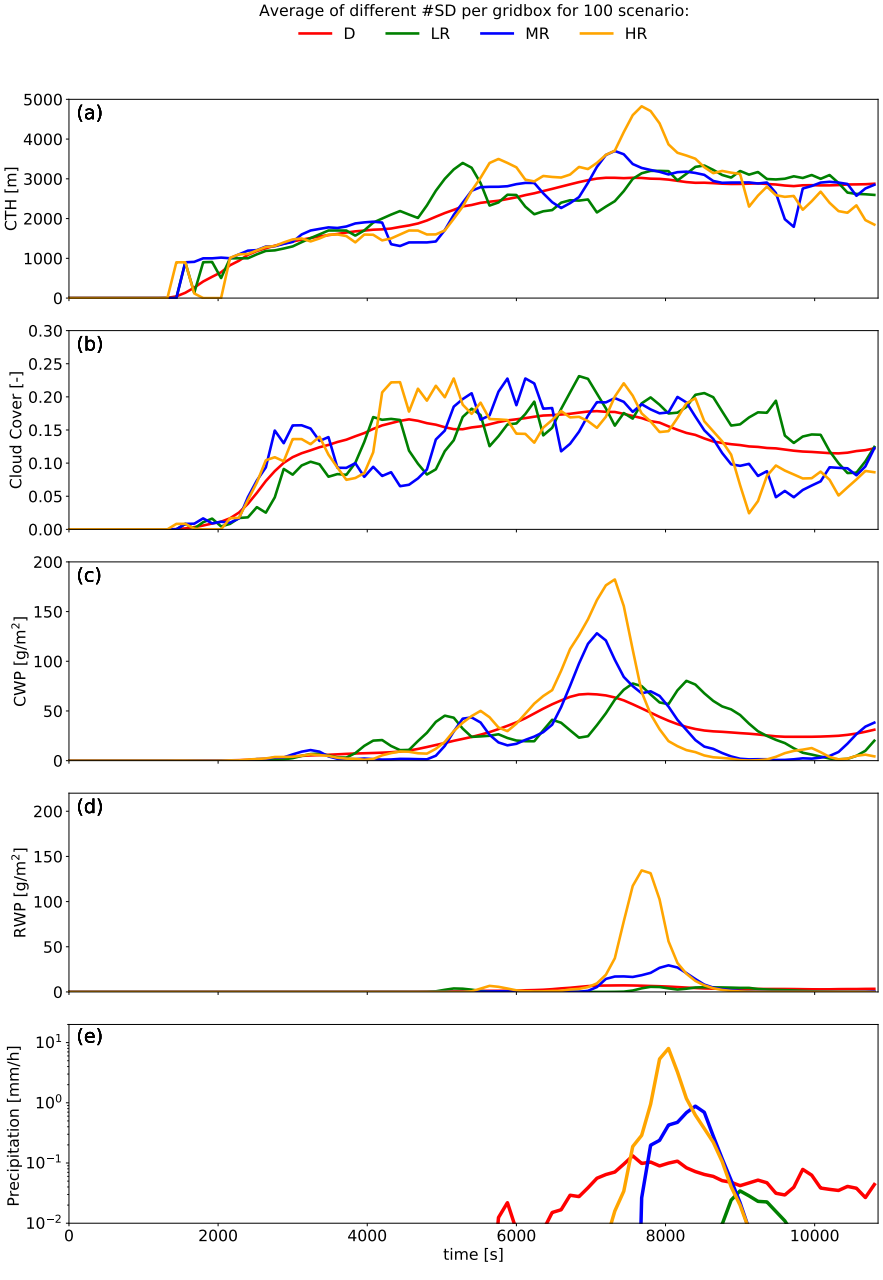

Figure 6. Time series of ensemble averages of cloud top height, cloud cover, cloud water path, rain water path and surface precipitation for D, LR, MR and HR scenarios with $N_{\mathrm{SD}}^{(\mathrm{bin})} = 100$. Cloud top height is the vertical position of the topmost cloudy cell. Cloud cover is the fraction of columns with at least one cloudy cell. Cloudy cells are cells with cloud water mixing ratio greater than 10^{-5}. Cloud droplets are droplets with $0.5\,\mu\mathrm{m} \leq r_w \leq 25\,\mu\mathrm{m}$. Rain drops are droplets with $25\,\mu\mathrm{m} \leq r_w$. Surface precipitation, CWP and RWP are domain averages divided by CC in order to obtain values representative of the cloudy area.

https://doi.org/10.5194/gmd-2023-44
Preprint. Discussion started: 12 April 2023

Geoscientific Model Development Discussions
Open Access
EGU

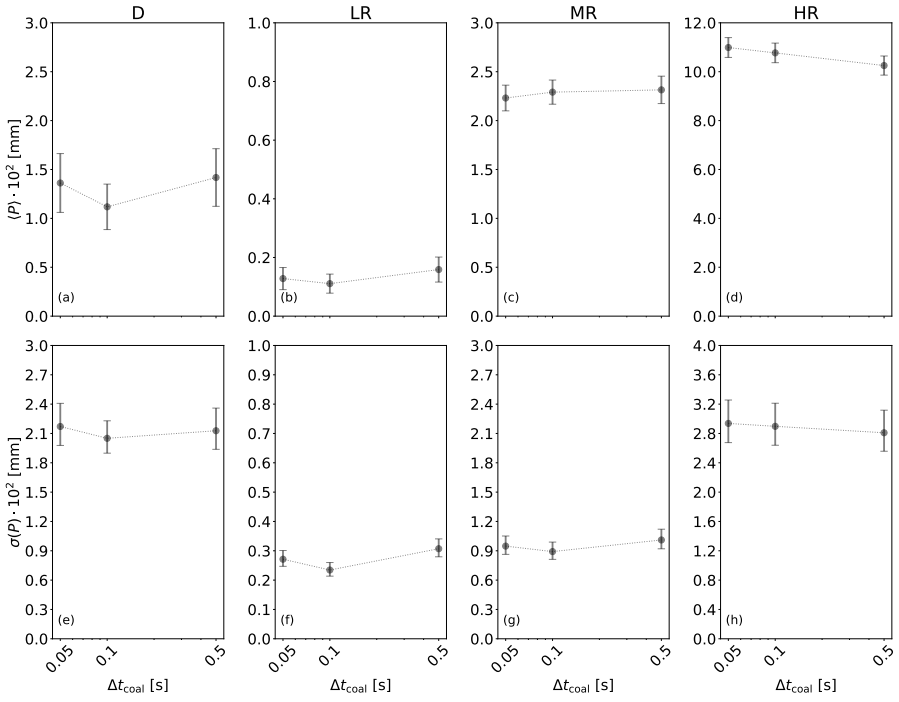

Figure 7. Ensemble mean and standard deviation of accumulated precipitation at the end of a simulation against time step for coalescence in four scenarios of a CC simulation with $N_{\mathrm{SD}}^{(\mathrm{bin})} = 100$. Error bars represent the 95% confidence interval.

Increase of $\langle P \rangle$ for $N_{\mathrm{SD}}^{(\mathrm{bin})} > 10^3$ in D, LR and MR cannot be explained by box simulations nor by CC simulations without collision-coalescence, because mean results in these types of simulations converge for $N_{\mathrm{SD}}^{(\mathrm{bin})} > 10^3$. This suggests that $\langle P \rangle$ may be affected by to large variance of the DSD, which does not converge even for $N_{\mathrm{SD}}^{(\mathrm{bin})} > 10^3$. The fact that $\langle P \rangle$ quickly convergence with Δt_{coal} supports this hypothesis, because Δt_{coal} does not affect the variance of the DSD. A potential mechanism linking DSD variance with precipitation includes erroneous spatial distribution of droplets and mixing of droplets between cells. Too large variance and correct mean of the DSD in box simulations corresponds to a situation in which in LES differences between DSD in neighbouring cells are larger than expected. There are some cells with more large droplets than expected, and some cells with less large droplets than expected. In an ensemble of independent boxes, these differences average out. However in 2D simulations, mixing brings together droplets from different cells. The fact that $\langle P \rangle$ slowly increases for $N_{\mathrm{SD}}^{(\mathrm{bin})} > 10^3$ suggests that a smoother spatial distribution of the DSD, together with mixing, may lead to more precipitation.

Spatial variance of the DSD is related to the ”lucky droplets” effect. ”Lucky droplets” are droplets that undergo series of unlikely collisions and grow faster than average. Some ”lucky” cells have more ”lucky droplets” and contain more large drops than most of the other cells. Increased variance in AON can be seen as an increased number of ”lucky droplets”. There is evidence that the increased variance negatively affects precipitation, indicating that the ”lucky droplets” effect may actually decrease the amount of rain.

https://doi.org/10.5194/gmd-2023-44
Preprint. Discussion started: 12 April 2023

Geoscientific Model Development Discussions

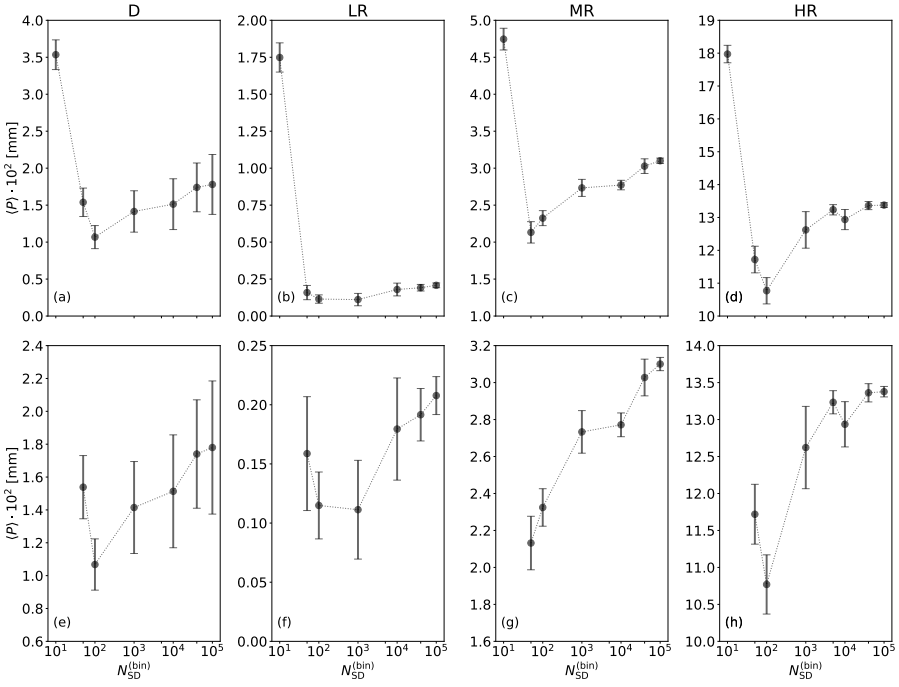

Figure 8. Ensemble mean of precipitation against number of super-droplets for four scenarios: D, LR, MR and HR. In (e-h) the same results are shown as in (a-d), but without $N_{\mathrm{SD}}^{(\mathrm{bin})} = 10$. Error bars show the 95% confidence interval.

4.6.2 Convergence of $\sigma(P)$ with $N_{\mathrm{SD}}^{(\mathrm{bin})}$

Standard deviation of precipitation for differing number of SDs is shown in fig. 9. In dynamic simulations (subplot a), $\sigma(P)$ is large for $N_{\mathrm{SD}}^{(\mathrm{bin})} = 10$, then sharply decreases for $N_{\mathrm{SD}}^{(\mathrm{bin})} = 50$ and does not change significantly as $N_{\mathrm{SD}}^{(\mathrm{bin})}$ is further increased. Most of the 95 % confidence intervals are overlapping for $N_{\mathrm{SD}}^{(\mathrm{bin})} \geq 50$. The relative standard deviation (subplot e) is around 1.5 for $N_{\mathrm{SD}}^{(\mathrm{bin})} \geq 50$, although there seems to be a (not statistically significant) decreasing trend for $N_{\mathrm{SD}}^{(\mathrm{bin})} \geq 10^4$. The relatively low sensitivity of $\sigma(P)$ to $N_{\mathrm{SD}}^{(\mathrm{bin})}$ in dynamic simulations shows that precipitation is more sensitive to differences in the flow field, which can be a consequence of small random perturbations of initial conditions, than to differences in realization of the collision-coalescence model of particle microphysics.

In kinematic simulations (subplots b-d) standard deviation of precipitation is more sensitive to $N_{\mathrm{SD}}^{(\mathrm{bin})}$ than in dynamic simulations. There is a significant decrease of $\sigma(P)$ as $N_{\mathrm{SD}}^{(\mathrm{bin})}$ is increased (except for small $N_{\mathrm{SD}}^{(\mathrm{bin})}$ in HR). The relative standard deviation has a maximum for $N_{\mathrm{SD}}^{(\mathrm{bin})}$ between 50 and 100, and decreases for higher $N_{\mathrm{SD}}^{(\mathrm{bin})}$ (subplots f-h). This shows that in the absence of differences in flow field, precipitation is governed by realizations of the collision-coalescence model. Comparing D with MR, which is the kinematic case with the most similar $\langle P \rangle$, we find that $\sigma(P)/\langle P \rangle$ in dynamic simulations is around 4 times higher than in kinematic simulations. This is another example of the fact that precipitation primarily depends on the realized flow field.

https://doi.org/10.5194/gmd-2023-44
Preprint. Discussion started: 12 April 2023

Geoscientific Model Development
Discussions
Open Access
EGU

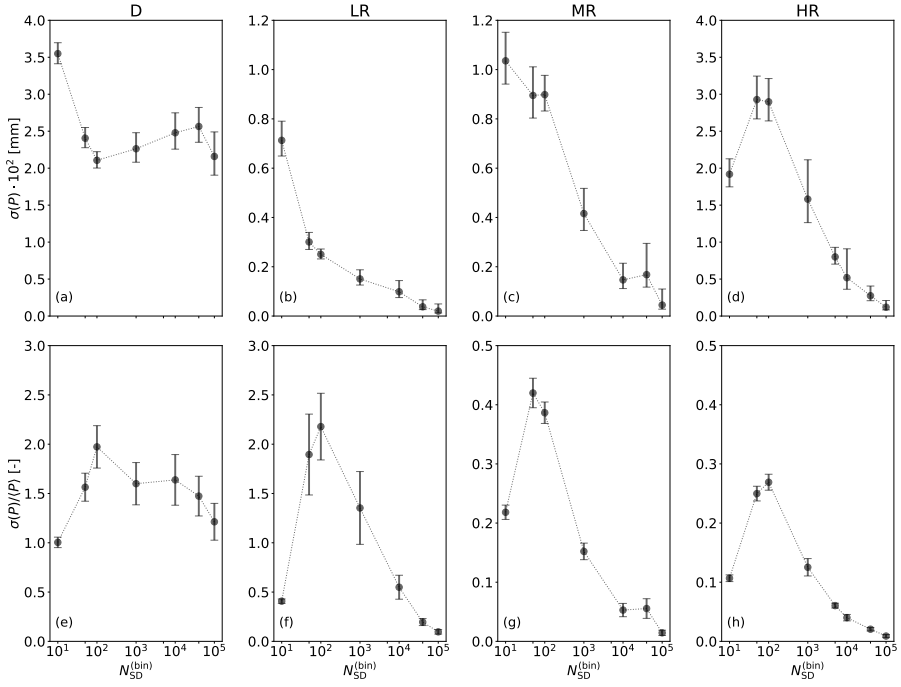

Figure 9. Ensemble standard deviation (a-d) and relative standard deviation(e-h) of precipitation against number of super-droplets for four types of simulations: D, LR, MR and HR. In (a-d), error bars show the 95% confidence interval. In (e-h), error bars show the error $\mathrm{e}(\sigma(P)/\langle P\rangle)$ estimated with: $\frac{\mathrm{e}(\sigma(P)/\langle P\rangle)}{\sigma(P)/\langle P\rangle} = \sqrt{\left(\frac{\mathrm{se}(\langle P\rangle)}{\langle P\rangle}\right)^2 + \left(\frac{\mathrm{se}(\sigma(P))}{\sigma(P)}\right)^2}$.

4.7 Sensitivity to SD initialization method

Collision-coalescence in particle microphysics is sensitive to the way SD attributes are initialized. Therefore the way precipitation changes with the number of SDs could depend on SD initialization. To check this, we test convergence for three types of SD initialization that were introduced in section 2.1: ξ_{const}-init, "const SD"-init and "const SD" fixed-init. In "const SD" fixed-init the outermost bin edges for dry radius were set to $1\,\mathrm{nm}$ and $5\,\mu\mathrm{m}$. Comparison of results for different initialization methods in the HR case is shown in fig. 10. We see only minor differences between "const SD"-init and "const SD" fixed-init. Both methods use bins to make sampling of the initial aerosol radius more even, but differ in the way the entire bin range is selected. Recently, Hill et al. (2023) found differences in precipitation between different implementations of particle microphysics, both using AON and binned initialization. Differences in details of bin initialization were proposed as one of potential reasons for the observed discrepancies. Good agreement between "const SD"-init and "const SD" fixed-init in our simulations suggests that some other factor is responsible for the discrepancies discussed in Hill et al. (2023).

The ξ_{const}-init gives much different results than bin methods. In ξ_{const}-init there is very little precipitation when $N_{\mathrm{SD}}^{(\mathrm{init})}$ is small. As more SDs are used the amount of precipitation increases. It is plausible that all methods of initialization should

https://doi.org/10.5194/gmd-2023-44
Preprint. Discussion started: 12 April 2023

Geoscientific Model Development Discussions

converge for large enough number of SDs. However, even for $N_{\mathrm{SD}}^{(\mathrm{init})} = 10^4$, which was the largest number of SDs that we were able to model in ξ_{const}-init, ξ_{const}-init gives less precipitation than the other methods. Unterstrasser et al. (2017) showed that ξ_{const}-init requires a huge number of SDs in box simulations of collision-coalescence and the authors hypothesized that it may require fewer SDs in cloud simulations. Our results show that this is not the case: in 2D simulations ξ_{const}-init has the same deficiencies as in box simulations. It requires a very large number of super-droplets, unattainable in 3D LES, to get convergence in precipitation. For fewer SDs it gives significantly too little precipitation.

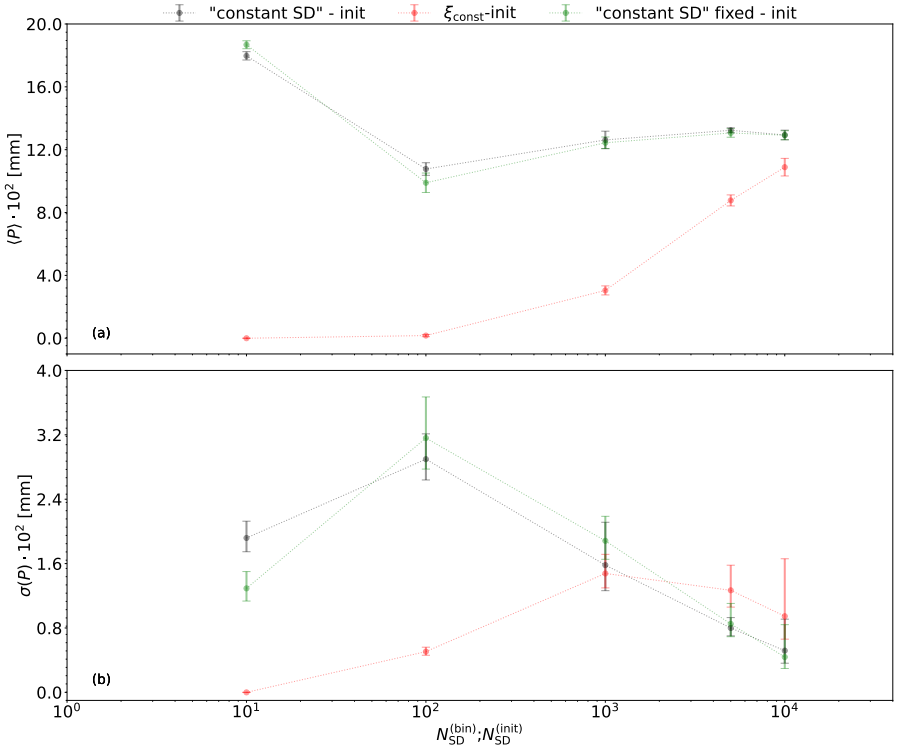

Figure 10. Mean $\langle P \rangle$ and standard deviation $\sigma(P)$ of accumulated precipitation against the number of SDs for HR simulations with three SD initialization methods. Horizontal axis is $N_{\mathrm{SD}}^{(\mathrm{bin})}$ in "constant SD"-init and $N_{\mathrm{SD}}^{(\mathrm{init})}$ in ξ_{const}-init. In "constant SD" fixed-init we have $N_{\mathrm{SD}}^{(\mathrm{init})} = N_{\mathrm{SD}}^{(\mathrm{bin})}$. Error bars represent the 95% confidence interval.

5 Conclusions

Our study shows that using particle microphysics it is more difficult to reach numerical convergence of precipitation in cloud simulations, even for a fixed flow field, than it is to reach convergence of mean DSD in an ensemble of box simulations of collision-coalescence. In general, convergence requirements are less strict in strongly precipitating clouds than in lightly precipitating clouds.

https://doi.org/10.5194/gmd-2023-44
Preprint. Discussion started: 12 April 2023


Geoscientific Model Development Discussions

It is relatively easy to have convergence with Δt_{coal}. Mean precipitation in our isolated cumulus simulations converged for $\Delta t_{\mathrm{coal}} = 0.5\,\mathrm{s}$. The same time step length was also sufficient in simulations of cumulus cloud fields (Dziekan et al., 2021). However, box simulations presented in this text and stratocumulus cloud field simulations from Dziekan et al. (2021) required $\Delta t_{\mathrm{coal}} = 0.1\,\mathrm{s}$. This suggests that $\Delta t_{\mathrm{coal}} = 0.1\,\mathrm{s}$ is a safe choice for cloud modeling. We used the linear sampling technique. Quadratic sampling may allow for longer time steps (Unterstrasser et al., 2020). Variance of precipitation in cloud simulations and variance of the DSD in box simulation are not sensitive to Δt_{coal}.

It is more difficult to reach convergence with the number of SDs per cell. In box simulations mean DSD converges for $N_{\mathrm{SD}}^{(\mathrm{bin})} \geq 10^3$, but variance of the DSD decreases with $N_{\mathrm{SD}}^{(\mathrm{bin})}$ without converging. In isolated cumulus simulations mean precipitation converges for $N_{\mathrm{SD}}^{(\mathrm{bin})} \geq 5 \times 10^3$, but only in the most heavily precipitating case. In cases with less precipitation we do not see convergence of mean precipitation. The maximum value studied was $N_{\mathrm{SD}}^{(\mathrm{bin})} = 10^5$. Typically, LES is done for $N_{\mathrm{SD}}^{(\mathrm{bin})}$ around 10^2. This study suggests that such simulations may underestimate surface precipitation, in particular in lightly precipitating clouds.

Lack of convergence of mean precipitation in cloud simulations despite convergence of mean DSD in box simulations for the same $N_{\mathrm{SD}}^{(\mathrm{bin})}$ suggests that mean precipitation is affected by too large spatial variance of the DSD within a cloud, which corresponds to too large variance of the DSD in an ensemble of box simulations. In other words, smaller (larger) differences between the DSD in neighbouring cells potentially give more (less) rain. It is interesting to note that in bin microphysics there is no variance in the DSD due to collision-coalescence and the DSD is smoothed by numerical diffusion. If the hypothesis that smooth spatial distribution of the DSD leads to more precipitation is true, LES with bin microphysics could be expected to give more precipitation than LES with particle microphysics, especially in lightly precipitating clouds.

Variance of precipitation in an ensemble of cloud simulations decreases with $N_{\mathrm{SD}}^{(\mathrm{bin})}$, but only if the same flow field is used in the ensemble. If the flow field is different in different simulations, e.g. due to random perturbations of initial conditions, variance of precipitation is not sensitive to $N_{\mathrm{SD}}^{(\mathrm{bin})}$. This shows that in typical LES the increased variance in the number of collisions in particle microphysics does not affect variability in rain between simulation runs, because differences in realized flow fields are more important.

Overall, this work shows how difficult it is to have numerical convergence of rain in LES of clouds. Further studies of collision-coalescence modeling in cloud simulations with particle microphysics are needed. One subject of interest would be to test convergence in another implementations of particle microphysics in order to validate our findings. Another subject would be to study spatial distribution of the DSD in particle microphysics in LES with varying resolution and the potential connection between smoothness of the spatial distribution and precipitation formation.

Author contributions. PZ and PD conceived the idea of the study. Simulations, analyses and data visualisation for CC were performed by PZ, for the box model by PD. All authors contributed to the manuscript. Funding were secured by PD and HP.

https://doi.org/10.5194/gmd-2023-44
Preprint. Discussion started: 12 April 2023


Geoscientific Model Development Discussions

Competing interests. No competing interests are present

Code and data availability. Cloud and box simulations were done using UWLCM and *coal_fluctu*, respectively. Both models use the SDM implementation from the *libcloudph++* library (Arabas et al., 2015). UWLCM also uses the *libmpdata++* library (Jaruga et al., 2015). Plotting of UWLCM results was done with the *UWLCM_plotting* package. In the study, the following code versions were used: UWLCM v2.1 (Dziekan et al., 2023), libmpdata++ v2.1 (Arabas et al., 2023b), libcloudph++ v3.1 (Arabas et al., 2023a), UWLCM_plotting v1.0 (Dziekan and Zmijewski, 2023), coal_fluctu v2.0 (Dziekan, 2023). Dataset, run scripts, and plotting scripts are available at Zmijewski et al. (2023).

Acknowledgements. This research was supported by the Polish National Science Center grant no 2018/31/D/ST10/01577, by the PLGrid Infrastructure, by the Interdisciplinary Centre for Mathematical and Computational Modelling of the University of Warsaw and by the Academic Computer Centre Cyfronet AGH.

https://doi.org/10.5194/gmd-2023-44
Preprint. Discussion started: 12 April 2023

References

Andrejczuk, M., Grabowski, W. W., Reisner, J., and Gadian, A.: Cloud-aerosol interactions for boundary layer stratocumulus in the Lagrangian Cloud Model, Journal of Geophysical Research Atmospheres, 115, https://doi.org/10.1029/2010JD014248, 2010.

Arabas, S. and Shima, S. I.: Large-eddy simulations of trade wind cumuli using particle-based microphysics with monte Carlo coalescence, Journal of the Atmospheric Sciences, 70, 2768–2777, https://doi.org/10.1175/JAS-D-12-0295.1, 2013.

Arabas, S., Jaruga, A., Pawlowska, H., and Grabowski, W. W.: Libcloudph++ 1.0: A single-moment bulk, double-moment bulk, and particle-based warm-rain microphysics library in C++, Geoscientific Model Development, 8, 1677–1707, https://doi.org/10.5194/gmd-8-1677-2015, 2015.

Arabas, S., Jaruga, A., Dziekan, P., Waruszewski, M., and Jarecka, D.: libcloudph++ v3.1 source code, https://doi.org/10.5281/zenodo.7643319, 2023a.

Arabas, S., Waruszewski, M., Dziekan, P., Jaruga, A., Jarecka, D., Badger, C., and Singer, C.: libmpdata++ v2.1 source code, https://doi.org/10.5281/zenodo.7643674, 2023b.

Arakawa, A. and Lamb, V. R.: Computational Design of the Basic Dynamical Processes of the UCLA General Circulation Model, General circulation models of the atmosphere, 17, 173–265, https://doi.org/10.1016/b978-0-12-460817-7.50009-4, 1977.

Bott, A.: An efficient numerical flux method for the solution of the stochastic collection equation, Journal of Aerosol Science, 28, 2284–2293, https://doi.org/10.1016/S0021-8502(97)85371-2, 1997.

Davis, M. H.: Collisions of Small Cloud Droplets: Gas Kinetic Effects, Journal of the Atmospheric Sciences, 29, 911–915, https://doi.org/10.1175/1520-0469(1972)029<0911:coscdg>2.0.co;2, 1972.

Dziekan, P.: Coal Fluctu v2.0 source code, https://doi.org/10.5281/zenodo.7680762, 2023.

Dziekan, P. and Pawlowska, H.: Stochastic coalescence in Lagrangian cloud microphysics, Atmospheric Chemistry and Physics, 17, 13 509–13 520, https://doi.org/10.5194/acp-17-13509-2017, 2017.

Dziekan, P. and Zmijewski, P.: University of Warsaw Lagrangian Cloud Model (UWLCM) 2.0: adaptation of a mixed Eulerian–Lagrangian numerical model for heterogeneous computing clusters, Geoscientific Model Development, 15, 4489–4501, https://doi.org/10.5194/gmd-15-4489-2022, 2022.

Dziekan, P. and Zmijewski, P.: UWLCM plotting v1.0 source code, https://doi.org/10.5281/zenodo.7643747, 2023.

Dziekan, P., Waruszewski, M., and Pawlowska, H.: University of Warsaw Lagrangian cloud model (UWLCM) 1.0: A modern large-eddy simulation tool for warm cloud modeling with Lagrangian microphysics, Geoscientific Model Development, 12, 2587–2606, https://doi.org/10.5194/gmd-12-2587-2019, 2019.

Dziekan, P., Jensen, J. B., Grabowski, W. W., and Pawlowska, H.: Impact of Giant Sea Salt Aerosol Particles on Precipitation in Marine Cumuli and Stratocumuli: Lagrangian Cloud Model Simulations, Journal of the Atmospheric Sciences, 78, 4127–4142, https://doi.org/10.1175/JAS-D-21-0041.1, 2021.

Dziekan, P., Singer, C., Waruszewski, M., Jaruga, A., Piotr, GlazerMann, and Badger, C.: University of Warsaw Lagrangian Cloud Model v2.1 source code, https://doi.org/10.5281/zenodo.7643309, 2023.

Gillespie, D. T.: Exact Method for Numerically Simulating the Stochastic Coalescence Process in a Cloud., Journal of the Atmospheric Sciences, 32, 1977–1989, https://doi.org/10.1175/1520-0469(1975)032<1977:AEMFNS>2.0.CO;2, 1975.

Grabowski, W. W.: Comparison of eulerian bin and lagrangian particle-based microphysics in simulations of nonprecipitating cumulus, Journal of the Atmospheric Sciences, https://doi.org/10.1175/JAS-D-20-0100.1, 2020.

https://doi.org/10.5194/gmd-2023-44
Preprint. Discussion started: 12 April 2023

Grinstein, F. F., Margolin, L. G., and Rider, W. J.: Implicit large eddy simulation: Computing turbulent fluid dynamics, vol. 9780521869, Cambridge university press, https://doi.org/10.1017/9780511618604, 2007.

Hall, W. D.: A Detailed Microphysical Model Within a Two-Dimensional Dynamic Framework: Model Description and Preliminary Results, Journal of the Atmospheric Sciences, 37, 2486–2507, https://doi.org/10.1175/1520-0469(1980)037<2486:admmwa>2.0.co;2, 1980.

Hill, A. A., Lebo, Z. J., Andrejczuk, M., Arabas, S., Dziekan, P., Field, P., Gettelman, A., Hoffmann, F., Pawlowska, H., Onishi, R., and Vié, B.: Toward a Numerical Benchmark for Warm Rain Processes, Journal of the Atmospheric Sciences, -1, https://doi.org/10.1175/JAS-D-21-0275.1, 2023.

Hoffmann, F. and Feingold, G.: Cloud Microphysical Implications for Marine Cloud Brightening: The Importance of the Seeded Particle Size Distribution, Journal of the Atmospheric Sciences, 78, 3247–3262, https://doi.org/10.1175/JAS-D-21-0077.1, 2021.

Hoffmann, F., Raasch, S., and Noh, Y.: Entrainment of aerosols and their activation in a shallow cumulus cloud studied with a coupled LCM-LES approach, Atmospheric Research, 156, 43–57, https://doi.org/10.1016/j.atmosres.2014.12.008, 2015.

Jaruga, A., Arabas, S., Jarecka, D., Pawlowska, H., Smolarkiewicz, P. K., and Waruszewski, M.: Libmpdata++ 1.0: A library of parallel MPDATA solvers for systems of generalised transport equations, Geoscientific Model Development, 8, 1005–1032, https://doi.org/10.5194/gmd-8-1005-2015, 2015.

Khvorostyanov, V. I. and Curry, J. A.: Terminal velocities of droplets and crystals: Power laws with continuous parameters over the size spectrum, Journal of the Atmospheric Sciences, 59, 1872–1884, https://doi.org/10.1175/1520-0469(2002)059<1872:TVODAC>2.0.CO;2, 2002.

Lasher-Trapp, S. G., Knight, C. A., and Straka, J. M.: Early Radar Echoes from Ultragiant Aerosol in a Cumulus Congestus: Modeling and Observations, Journal of the Atmospheric Sciences, 58, 3545 – 3562, https://doi.org/10.1175/1520-0469(2001)058<3545:EREFUA>2.0.CO;2, 2001.

Lipps, F. B. and Hemler, R. S.: A scale analysis of deep moist convection and some related numerical calculations., Journal of the Atmospheric Sciences, 39, 2192–2210, https://doi.org/10.1175/1520-0469(1982)039<2192:ASAODM>2.0.CO;2, 1982.

Onishi, R., Matsuda, K., and Takahashi, K.: Lagrangian tracking simulation of droplet growth in turbulence-turbulence enhancement of autoconversion rate, Journal of the Atmospheric Sciences, 72, 2591–2607, https://doi.org/10.1175/JAS-D-14-0292.1, 2015.

Rao, C. R.: Linear Statistical Inference and its Applications, Wiley, https://doi.org/10.1002/9780470316436, 1973.

Riechelmann, T., Noh, Y., and Raasch, S.: A new method for large-eddy simulations of clouds with Lagrangian droplets including the effects of turbulent collision, New Journal of Physics, 14, 65 008, https://doi.org/10.1088/1367-2630/14/6/065008, 2012.

Sheskin, D. J.: Handbook of Parametric and Nonparametric Statistical Procedures, https://doi.org/10.1201/9780429186196, 2020.

Shima, S., Kusano, K., Kawano, A., Sugiyama, T., and Kawahara, S.: The super-droplet method for the numerical simulation of clouds and precipitation: A particle-based and probabilistic microphysics model coupled with a non-hydrostatic model, Quarterly Journal of the Royal Meteorological Society, 135, 1307–1320, https://doi.org/10.1002/qj.441, 2009.

Shima, S. I., Sato, Y., Hashimoto, A., and Misumi, R.: Predicting the morphology of ice particles in deep convection using the super-droplet method: Development and evaluation of SCALE-SDM 0.2.5-2.2.0, -2.2.1, and -2.2.2, Geoscientific Model Development, 13, 4107–4157, https://doi.org/10.5194/GMD-13-4107-2020, 2020.

Smolarkiewicz and Margolin, L. G.: Variational Methods for Elliptic Problems in Fluid Models, pp. 137–159, 2000.

Smolarkiewicz, P. K.: Multidimensional positive definite advection transport algorithm: an overview, International Journal for Numerical Methods in Fluids, 50, 1123–1144, https://doi.org/10.1002/fld.1071, 2006.

https://doi.org/10.5194/gmd-2023-44
Preprint. Discussion started: 12 April 2023

Sölch, I. and Kärcher, B.: A large-eddy model for cirrus clouds with explicit aerosol and ice microphysics and Lagrangian ice particle tracking, Quarterly Journal of the Royal Meteorological Society, 136, 2074–2093, https://doi.org/10.1002/qj.689, 2010.

Unterstrasser, S., Hoffmann, F., and Lerch, M.: Collection/aggregation algorithms in Lagrangian cloud microphysical models: Rigorous evaluation in box model simulations, Geoscientific Model Development, 10, 1521–1548, https://doi.org/10.5194/gmd-10-1521-2017, 2017.

Unterstrasser, S., Hoffmann, F., and Lerch, M.: Collisional growth in a particle-based cloud microphysical model: Insights from column model simulations using LCM1D (v1.0), Geoscientific Model Development, 13, 5119–5145, https://doi.org/10.5194/GMD-13-5119-2020, 2020.

VanZanten, M. C., Stevens, B., Nuijens, L., Siebesma, A. P., Ackerman, A. S., Burnet, F., Cheng, A., Couvreux, F., Jiang, H., Khairoutdinov, M., Kogan, Y., Lewellen, D. C., Mechem, D., Nakamura, K., Noda, A., Shipway, B. J., Slawinska, J., Wang, S., and Wyszogrodzki, A.: Controls on precipitation and cloudiness in simulations of trade-wind cumulus as observed during RICO, Journal of Advances in Modeling Earth Systems, 3, https://doi.org/10.1029/2011MS000056, 2011.

Zmijewski, P., Dziekan, P., and Pawlowska, H.: Data and scripts accompanying the paper "Modeling Collision-Coalescence in Particle Microphysics: Numerical Convergence of Mean and Variance of Precipitation in Cloud Simulations", https://doi.org/10.5281/zenodo.7685539, 2023.